Response of Delta Modulation to Gaussian Signals

By M. R. AARON, J. S. FLEISCHMAN, R. A. McDONALD, and E. N. PROTONOTARIOS

(Manuscript received October 30, 1968)

Analytical, experimental, and computer simulation results are given for the error spectrum of a delta modulator when probed by stationary, band limited, gaussian noise. These three complementary methods are used to increase our quantitative understanding of the nonlinear system with memory. The error is conveniently split into two components: one linearly dependent on the input signal and one linearly independent of the input signal. In order to isolate these two types of errors we use two measurement techniques. For purposes of analysis we show that the delta modulator can be replaced by an equivalent linear system with additive noise at its output which is linearly uncorrelated with the input. The equivalent linear system may be approximated by using methods involving statistical linearization or the deterministic describing function. Alternately, the equivalent linear system may be obtained from computer simulation.

I. INTRODUCTION

1.1 *General Background and Broad Objectives*

Delta modulation (DM) has been known for almost two decades; yet, little has been published comparing experiment with theory particularly for random inputs.† On the surface this might seem strange because of the apparent simplicity of the delta modulation system blocked out in Fig. 1(a). The waveforms depicted in Fig. 1(b) and the mathematical model in Fig. 1(c) should suffice to explain how the system operates. The principal difficulty of the analysis is the absence of general tools for handling random processes in nonlinear systems with memory. From this viewpoint the simplicity of the delta

† The first reference to delta modulation appeared in French patent literature (see Ref. 1) in 1946, but the first readily available description in English appeared in 1952 (see Ref. 2).

modulator is deceptive. However, if we make some inroads into the quantitative understanding of this seemingly simple case, it may give us courage to go on to more complicated situations.

In this paper we concentrate on the development and exploitation of analytical, experimental, and computational techniques to enhance our understanding of the objective performance of delta modulation. We do not consider the correlation of objective measures with subjective effects for applications to either voice or video; rather, our main aim is to correlate what is known in theory, including our own developments with what has been achieved experimentally.

Renewed interest has come from at least two sources. First, differential systems of which delta modulation is the simplest member, have long been known to be well suited to handling signals whose spectra fall off at high frequencies.[3–5] This is particularly true of black and white video; there is substantial interest in transmitting such signals digitally.[6] Interest also has been generated by the desire to produce inexpensive time division switching and transmission systems for voice.[7] In this application, delta modulation is attractive because of its simplicity and great compatibility with the emerging integrated circuit technology.

1.2 *Use of the Random Noise Probe*

Reasons for characterizing a delta modulator with a random noise probe are twofold. First, the envelope of a scanned video signal has a power spectral density that is close to that obtained by passing gaussian noise through an RC filter.† Therefore objective performance measures obtained in response to this signal bear some relationship to subjective performance. Second, use of the established noise-loading procedure for determining the spectrum of the noise in a nonlinear system yields a "signature" that is useful for verifying that the delta modulator is performing as designed. Verification of prescribed performance is an essential prelude to careful subjective testing as well as an absolute necessity for production control. To avoid measurement problems that result from the low spectral density of the RC noise source at the upper end of the band, we deal with flat band-limited white noise almost exclusively.

1.3 *Chronology and Summary*

At the start of our work the signal-to-noise ratios obtained by computer, experiment, and analysis disagreed substantially, partic-

† We use the terms power spectral density, power spectrum, and spectrum interchangeably throughout.

ularly when the signal was changing more rapidly than the delta modulator could follow. In this region, known as the region of slope overload, two methods of computing slope overload noise differed markedly.[6,8] Reference 9 gives a reconciliation of the differences and the development of an analytical expression for the mean square value of the slope overload noise. By using the best features of the previous conflicting theories, an analytical result was obtained that yielded good agreement with computer results.[9] Granular noise, as computed from Van de Weg's approach, agreed with both simulation and experiments.[10] Results obtained by noise-loading experiments continued to disagree with both theory and simulation in the slope overload region. It quickly became apparent that the difference resulted from the fact that this measurement procedure did not measure the noise as defined by theory.

To clarify the differences it is desirable to consider the spectrum of the noise introduced by the delta modulator. Two definitions of noise are possible; the simplest is that the noise is the error, that is, the difference $[x(t) - y(t)]$ between the input signal and the local output signal as defined in Fig. 1. This error is correlated statistically with the input signal. In other words, the error may be considered to be made up of two components, one linearly dependent on the input signal and one linearly independent of the input signal. The linearly dependent component may be regarded as being caused by passing the signal through a noise-free linear filter.

This equivalent linear filter does not introduce noise but merely introduces frequency distortion, as for example in producing selective attenuation and phase shift, particularly for the higher frequency components of the signal that the delta modulator cannot follow. The noise component linearly independent of the signal may be viewed as equivalent to additive uncorrelated noise just as in the case of a nonfeedback type of pulse code modulation quantizer.[11] When the noise is split up this way, the components have distinctly different subjective effects and are thus meaningfully studied separately. In fact the spectrum of the uncorrelated component of the noise is measured by the noise-loading test pictured schematically in Fig. 2. This test procedure is commonly used to test transmission systems, primarily for nonlinear distortion, in this manner.[12] With the switch in the upper position, the colored gaussian noise is passed through a narrowband elimination filter prior to exciting the system under test. At the system output, noise generated by system nonlinearities is measured by the bandpass filter in the receiver of the noise-loading set. This

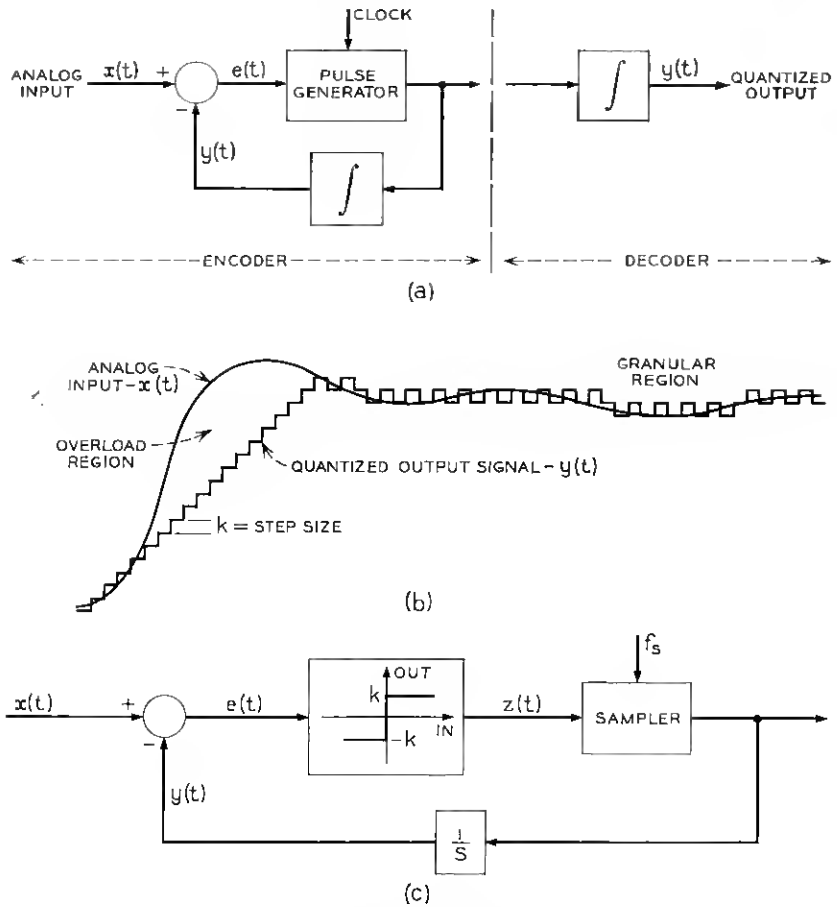

Fig. 1 — Delta modulation: (a) delta modulation system, (b) waveforms, (c) mathematical model.

filter passes only those frequency components eliminated from the input signal. This differs from the total noise as computed by analysis and simulation.

Two approaches were taken to reconcile measurements with the paper and pencil results. First, we used a straight-forward, but tedious, measurement procedure called the cancellation test to measure the total noise as defined by theory, that is, the difference between output and input. The results achieved substantiated the theoretical results. Unfortunately the cancellation or "feed-around" technique, as discussed in detail in Section IV, is tedious and difficult to perform ac-

eurately. This made it necessary to rely on the more convenient noise loading measurements. To compare theory and experiment it became necessary to remove the correlated components of the noise as obtained from theory and simulation. It was not possible to do so for the purely theoretical approach, but the results of the simulation were modified, as described in Section III, to agree with the measurement made with the noise-loading technique.

The equivalent linear filter, defined in Section 1.4, cannot be obtained analytically, but it may be determined using computer simulation. An approximate analytical method for arriving at the equivalent linear filter is statistical linearization to replace the quantizer (signum function, threshold circuit) of Fig. 1 with a "suitable" linear gain. This approach is discussed in Section 2.2 where comparisons are made of the equivalent linear filters obtained by the statistical linearization and simulation approaches. Most of the manipulations regarding the statistical linearization are relegated to Appendix A. Section 2.3 is concerned with harmonic analysis useful in its own right as well as a part of the cancellation test. The prelude to the Fourier analysis relevant to the sinusoidal response in the overload region is given in Appendix B.

In Section III we cover the highlights of the simulation program with emphasis on the spectral calculations. Estimates of accuracy are given in Section 3.2. Section IV is devoted to a discussion of the techniques used for measuring the spectrum of the error. We also show how the delta modulator parameters are measured and discuss the realization of a laboratory model delta modulator. Throughout the paper we compare experiment with theory and simulation. In Section V we make some general comments about the various sets of results.

1.4 *System Definition, Terminology, and Symbols*

The following are the terms and symbols used. Our input signal $x(t)$ in Fig. 1 is chosen from a stationary, zero mean, gaussian random process, band-limited to f_b. Its correlation function is $R_{xx}(\tau)$ and cor-

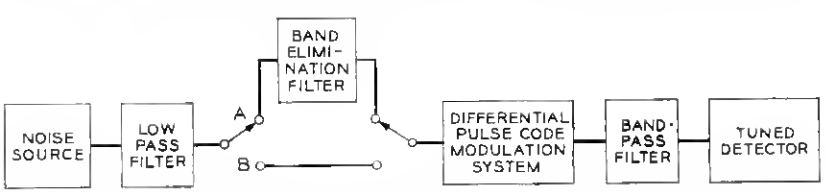

Fig. 2 — Noise loading test: When the switch is at A the uncorrelated noise is measured; when at B the signal plus total noise is measured.

responding spectral density $S_{xx}(\omega)$. The delta modulator is characterized by the step size k of the quantizer, sampling frequency f_s, or normalized sampling frequency $f_s/f_b = F_s$, and an ideal integrator with transfer function $1/s$.† Clearly the maximum slope that the delta modulator can follow is $kf_s \equiv x_o'$, which corresponds to a string of one's at its output. As k approaches zero with x_o' fixed, the granular noise tends to zero and the noise primarily results from slope overload. Under these conditions it will be convenient and quite accurate to represent the delta modulator as a continuous feedback loop with a step size x_o'. We make this assumption in much of the analysis to follow.

Throughout we use $e(t)$ for the total noise, $n(t)$ for that component of the noise uncorrelated with the input signal, $z(t)$ for the unsampled output of the threshold circuit, and $y(t)$ for the output of both the local integrator and the remote integrator (error free transmission). Other symbols are defined as needed.

II. DEFINITION OF THE UNCORRELATED NOISE—AN EQUIVALENT LINEAR SYSTEM

2.1 *General*

In this section we define an equivalent linear system and an additive uncorrelated noise which produce statistical behavior identical with that of the delta modulator up to second moments. Notice that any time invariant linear transformation of the input signal contained in the output may be considered as useful signal because, at least in principle, the input may be recovered by passing it through a fixed linear filter corresponding to the inverse linear transformation.

Definition 1: Equivalent Linear System. We compare the output of the delta modulator $y(t)$ with the output of an "equivalent linear system," defined by Figure 3, whose impulse response $g(t)$ is defined such that the difference

$$y(t) - g(t)*x(t) \triangleq n(t) \tag{1}$$

is uncorrelated with the input $x(t)$; that is,

$$R_{xn}(\tau) = \langle x(t+\tau)n(t)\rangle_{av} = \langle x(t+\tau)[y(t) - g(t)*x(t)]\rangle_{av} = 0 \tag{2}$$

where $*$ denotes convolution.

Definition 2: Additive Uncorrelated Noise. The difference $n(t)$

† In Section 2.2 we consider the more practical case of a leaky integrator with transfer function $1/(s + a)$.

given in equation (1), with equation (2) satisfied, is defined as the additive uncorrelated noise. Equation (2) is satisfied when

$$R_{xx}(\tau)*g(-\tau) = R_{xy}(\tau). \tag{3}$$

Taking the Fourier transforms of both sides of this equation and then the complex conjugates we get

$$G(j\omega) = \frac{S_{yx}(\omega)}{S_{xx}(\omega)} = 1 - \frac{1}{S_{xx}(\omega)} \{\text{Re}\,[S_{xe}(\omega)] - j\,\text{Im}\,[S_{xe}(\omega)]\}. \tag{4}$$

We remark here that the transfer function $G(j\omega)$ does not have to be causal; that is, $g(t)$ may be nonzero for $t < 0$.

Applying the orthogonality principle we can see that $g(t)$, thus found, also satisfies†

$$\langle [y(t) - g(t)*x(t)]^2 \rangle_{\text{av}} = \text{minimum}.$$

Notice that from Fig. 3, we can write

$$S_{yy}(\omega) = |\, G(j\omega)\,|^2\, S_{xx}(\omega) + S_{nn}(\omega). \tag{5}$$

If the input process $[x(t)]$ has a spectrum $S_{xx}(\omega)$ such that

$$S_{xx}(\omega) = 0 \quad \text{for} \quad \omega \,\varepsilon \left\{\omega_o - \frac{\Delta\omega}{2}\,,\, \omega_o + \frac{\Delta\omega}{2}\right\} \tag{6}$$

where ω_o is a given radian frequency and $\Delta\omega$ a small radian frequency slot, then applying (5) we get

$$S_{nn}(\omega) = S_{yy}(\omega) \quad \text{for} \quad \omega \,\varepsilon \left\{\omega_o - \frac{\Delta\omega}{2}\,,\, \omega_o + \frac{\Delta\omega}{2}\right\}. \tag{7}$$

So that for the noise power in this frequency slot we will have

$$\frac{1}{2\pi} \int_{\omega_o - \Delta\omega/2}^{\omega_o + \Delta\omega/2} S_{nn}(\omega)\, d\omega = \frac{1}{2\pi} \int_{\omega_o - \Delta\omega/2}^{\omega_o + \Delta\omega/2} S_{yy}(\omega)\, d\omega. \tag{8}$$

The noise-loading measurement described in Section I applies the technique mentioned here. Thus the noise spectrum and noise power measured are $S_{nn}(\omega)$ and $\langle n^2(t) \rangle_{\text{av}}$. In order to compare experiment and analysis we have to find $G(j\omega)$ and $\langle n^2(t) \rangle_{\text{av}}$. When we are slightly in slope overload, $G(j\omega)$ is practically equal to 1 and all noise definitions so far used are equivalent. When well into slope overload,

† Kazakov used this approach to obtain $g(t)$ or equivalently $G(j\omega)$ in equation (4) in 1960.[13] We were unaware of his work at the time we conceived of the additive uncorrelated noise approach which for our purposes has real physical appeal.

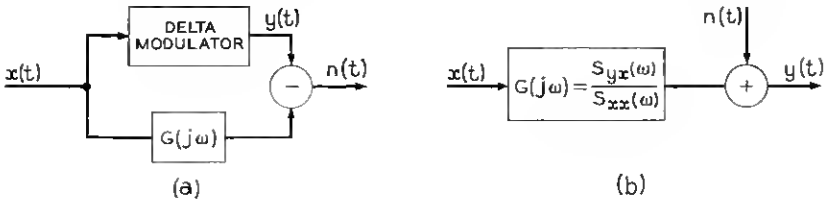

Fig. 3 — Equivalent linear system.

$G(j\omega)$ deviates markedly from unity, thus accounting for the differences between experiment and analysis. To find $G(j\omega)$ we need the cross-spectrum $S_{yx}(\omega)$ which is not presently available analytically. We can find $S_{yx}(\omega)$ using computer simulation; this is what is done in Section III.

2.2 *The Method of Statistical Linearization*

Even though the equivalent transfer function $G(j\omega)$ cannot be found analytically, it may be approximated through the method of statistical linearization.[14] Statistical linearization can be applied to the corresponding continuous system (without sampling) as shown in Fig. 4. The study of the slope overload noise corresponds to the study of this feedback loop, with the nonlinear element in the forward path being a hard limiter with saturation levels $\pm x'_0 = \pm kf_s$. The use of the continuous system is not a substantial limitation since the correlated component of the overall noise $e(t)$ is conjectured to be mainly overload noise.

The nonlinearity in the loop will be replaced by a linear gain K chosen according to criteria given in this section and in Appendix A. Independent of the choice of criterion, the equivalent linear system will have the form,

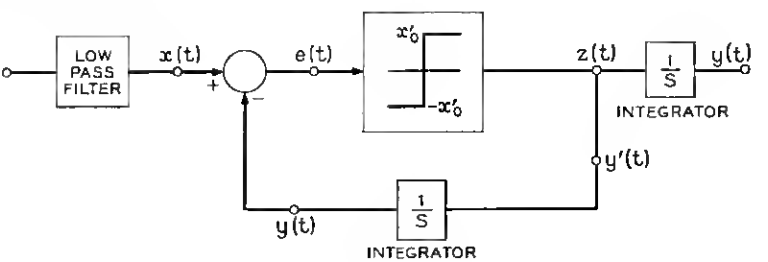

Fig. 4 — Continuous feedback system for the study of slope overload noise.

$$H(f) = A/(s + A) \tag{9}$$

or

$$H(f) = \frac{1}{1 + j(f/f_c)} \tag{10}$$

where f_c is the corner frequency (3dB frequeney) of the filter ($f_c = K/2\pi$).

In a real system, we generally have a leaky integrator whose transfer function is of the form $1/(s + a)$. Then it is easy to show that

$$H(f) = \frac{H(0)}{1 + j\dfrac{f}{f_c}} \tag{11}$$

where

$$H(0) = \frac{K}{K + a}, \quad \text{and} \quad f_c = \frac{K + a}{2\pi}.$$

The variety of ways by which one can determine the equivalent gain K, are presented in detail in Appendix I. Let us call K_1 the equivalent gain found with the assumption that the input to the nonlinearity is gaussian with variance σ^2 equal to the overload noise power. Denote by K_2 the equivalent linear gain wben the gaussian assumption is removed. Let K_3 be the equivalent gain determined under thc requirement that the differenee between the overload error and the input to the linearized element be uneorrelated (for $\tau = 0$) with the input signal. In order to eompare the equivalent linear filter transfer functions with the computer simulation results we plot the magnitude $| G(j\omega) |$ of the transfer function [calculated using equation (4) and thc computer genernted cross-spectra] for $kf_s/f_b = kF_s = 2$ and 4 in Fig. 5. From these figures we find that the equivalent linear system may bc approximated by a one-pole tranfer function with corner frequency, $f_c = 0.358\ f_b$ and $0.94\ f_b$, respectively, and corresponding dc gains (caused by the small leak in the integrators) $H(0) = 0.89$ and 0.98. The results of the eomparison are summarized in Table I. Thus there is reasonable agreement between the equivalent linear system transfer function obtained from computer simulation and all the approximate statistieal linearization methods.

2.3 *Describing Function Method*

In Appendix B a metbod is outlined for obtaining an equivalent frequency dependent complex gain for a delta modulation system with

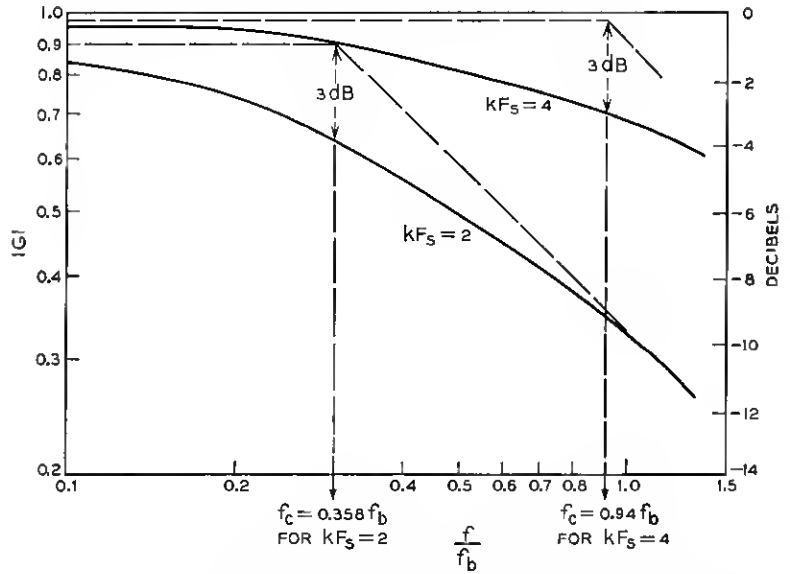

Fig. 5 — Bode plot of the gain of the equivalent linear system (computer results, $a = 0.16\ \omega_b$).

a leaky integrator, subject to a sinusoidal input of amplitude X_o and frequency ω_o, under pure slope overload conditions. This complex gain is defined to be the ratio of the complex amplitude of the fundamental of the output to the complex amplitude of the input sinusoid. This deterministic equivalent linearization method is well known as the describing

TABLE I—PARAMETERS OF EQUIVALENT LINEAR SYSTEMS

	$kF_s = 2$		$kF_s = 4$	
	K/f_b Equivalent linear gain	f_c/f_b Corner frequency	K/f_b Equivalent linear gain	f_c/f_b Corner frequency
Computer	$K_0 = 2.10$	0.358	$K_0 = 5.90$	0.94
Gaussian assumption	$K_1 = 2.34$	0.398	$K_1 = 7.13$	1.13
Without gaussian assumption	$K_2 = 1.48$	0.262	$K_2 = 4.00$	0.64
Correlated noise† Approach	$K_3 = 2.70$	0.43	$K_3 = 5.90$	0.94

† The leaky integrator effect is neglected; if taken into account the results would be somewhat smaller. For $kF_s = 4$, the effect of leak is negligible.

function method. The corresponding magnitude of the equivalent gain is given as a function of "normalized" frequency ($\omega_o X_o/x_o'$) in Fig. 6 when the leak in the integrator goes to zero. For $x_o' = kF_s = 2$ the 3 dB point (corner frequency) is at $f_c \cong 0.4 f_b$, which is in good agreement with the results in Table I. Measured values of equivalent gain shown on Fig. 6 agree well with theoretical predictions.

III. COMPUTER SIMULATION TECHNIQUE

3.1 *Basic Concepts*

Computer simulation provides a convenient method of studying the characteristics of delta modulation systems without actually building them. The computer can also provide accurate numerical results against which to compare experimental results from laboratory or

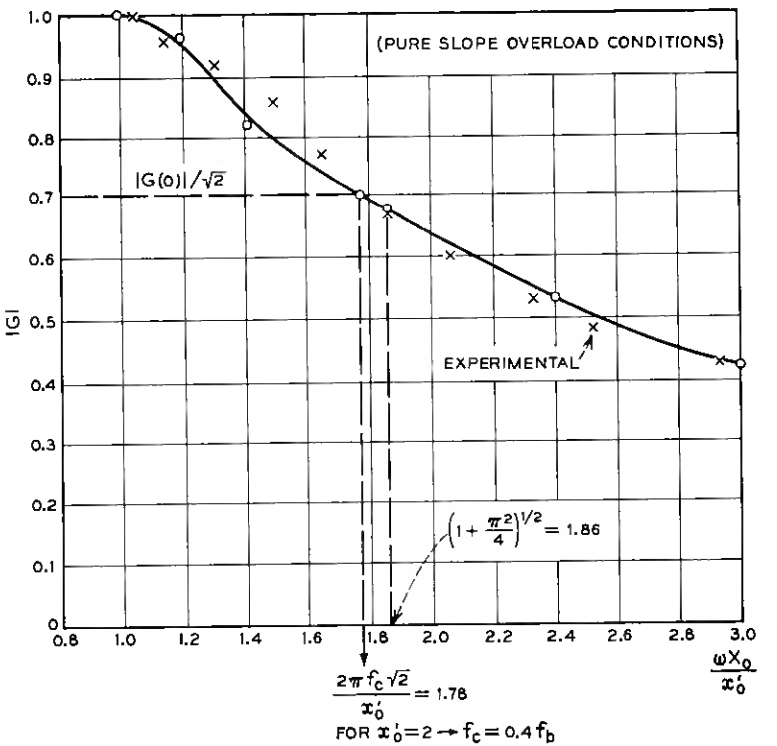

Fig. 6 — Harmonic response equivalent gain of a single integration ΔM.

production models. Computer simulation is a compromise between laboratory techniques and analytical techniques in that it is easy to change the program in order to study a variety of system parameters or to introduce defects similar to those expected in practical systems. On the other hand, the simulated system is an idealized abstraction which does not represent the practical system in full detail.

The BLØDI programming system, used for the simulation, results in a program which processes a sequence of samples by whatever set of mathematical operations may be specified by a block diagram.[15] BLØDI flexibility allows the use of FORTRAN for such things as computing estimates of signal statistics, for which FORTRAN is more efficient. Figure 7 indicates the basic philosophy: a FORTRAN program supervises the entire operation calling the various subprograms as needed. By structuring the simulation programs as a hierarchy of modules, changes in one area of the model could be effected without involving the entire program. The program was purposely written with extensive use of subroutines. This for example, makes it applicable to differential pulse code modulation (DPCM) by simply changing the subroutine for the quantizer. The actual programs are of interest to only a few people, and are not listed here. Appendix C gives a discussion of the computational formulas used to estimate correlation functions and spectra.

3.2 *Accuracy of Computer Estimates of Spectrum of Error*

In order to estimate the expected accuracy of the spectrum estimates from the computer simulation, the following example is given: In the simulation the estimate $S_e(k)$ is made on the basis of 10,000 input samples. Here k is an integer index related to frequency, and

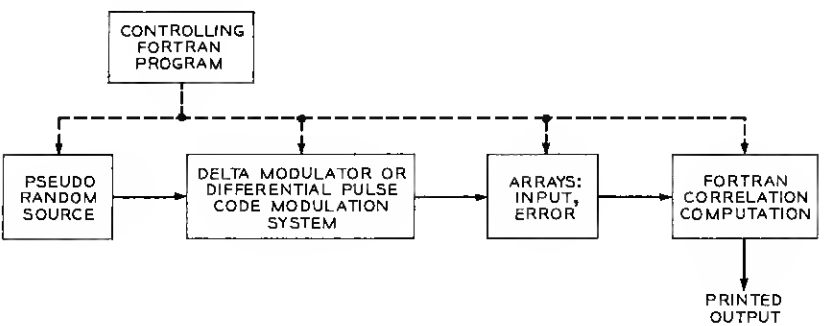

Fig. 7 — Computer simulation.

the subscript e refers to the total noise $e(t)$. In one particular run, ten intermediate estimates based on 1,000 input samples each were made. Using the notation $S_{e1}(k)$ through $S_{e10}(k)$ for these we have

$$\text{sample mean} = S_e(k) = \tfrac{1}{10}[S_{e1}(k) + \cdots + S_{e10}(k)] \tag{12}$$

$$E[S_e(k)] = \mu,$$

$$\text{sample variance} = \text{var} = \tfrac{1}{10}\{[S_{e1}(k) - S_e(k)]^2 + \cdots + [S_{e10}(k) - S_e(k)]^2\}. \tag{13}$$

One can then show that the variance of the estimate $S_e(k)$ relative to μ is estimated by

$$E\{[S_e(k) - \mu]^2\} = \tfrac{1}{9}\,\text{var}. \tag{14}$$

For the cancellation technique and one particular value of k, representing a low frequency point in the spectrum, a numerical computation yielded:

$$\frac{(\frac{1}{9}\,\text{var})^{\frac{1}{2}}}{S_e(k)} = 0.066.$$

Although the result may in general depend on k, spot checks at other points yielded similar results.

Assuming the estimate is a gaussian random variable with 0.066 = the ratio of standard deviation to mean, the result indicates that the estimate is within $\pm\frac{1}{2}$ dB of the true mean with probability 0.9.

Other sources that could contribute errors in the results of the simulation include: (*i*) random error in measurements caused by finite averaging time constant, estimated as $\pm\frac{1}{2}$ dB, (*ii*) round-off errors in computation, which are most significant in the region of high noise, and (*iii*) systematic error resulting from differences between the spectral shape of the simulated input and the output of the laboratory noise generator used in the experiments.

IV. EXPERIMENTAL TECHNIQUES

The extensive analytical and computer work that has been presented was undertaken to a large extent to gain a better understanding of an actual laboratory delta modulation system.

4.1 *Description of the Delta Modulator*

The delta modulator used for the measurements is a variable parameter system in which the step size, leak, and sampling rate are

independently variable. Figure 8 is a block diagram of the encoder. The difference between the input and the local integrator output is amplified and presented to the threshold detector. This circuit controls the output of the pulse generator.

The local integrator has circuit elements which can be changed to vary the important parameters of the system. The capacitor C controls the step size; since the amplifier has a high input impedance, the resistor R_L controls the leak.

The decoder consists of a regenerator for amplitude and phase regeneration and a decoder integrator which is a duplicate of the local integrator. The system was operated at a 12.5 MHz sampling rate.

Waveforms in a delta modulator are rather simple; nevertheless, some are shown in Fig. 9 to illustrate the actual operation of the system. Figure 9a indicates the output of the decoder and the pulse output of the coder when no input is presented to the system. A delta modulator should change state every clock period with no input; the photograph illustrates this. This waveform can be used to measure the step size.

Figure 9b illustrates the output of the system when it is in overload. The slope of the input sinusoidal signal is greater than the slope that the delta modulator can follow. Therefore, the output is a triangular wave whose slope is a measure of the normalized step size. An interesting feature can be seen by observing the slopes of the flat steps in this picture. In the lower half, they slant upward and in the upper half they slant downward, illustrating the leaking off of the capacitor voltage.

Figure 9c illustrates the response of the delta modulator to a sine wave whose amplitude is below overload. The rather blurred trace

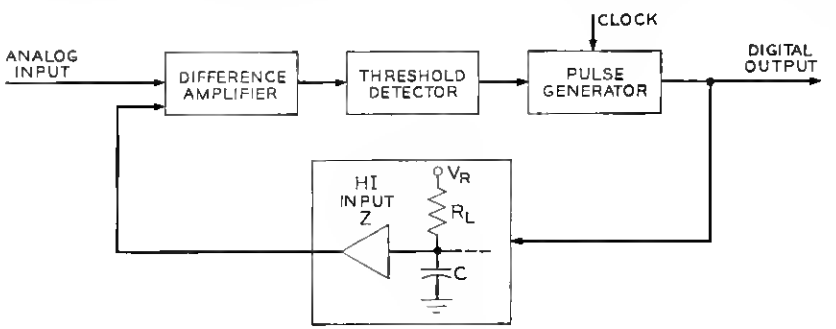

Fig. 8 — Delta modulator encoder.

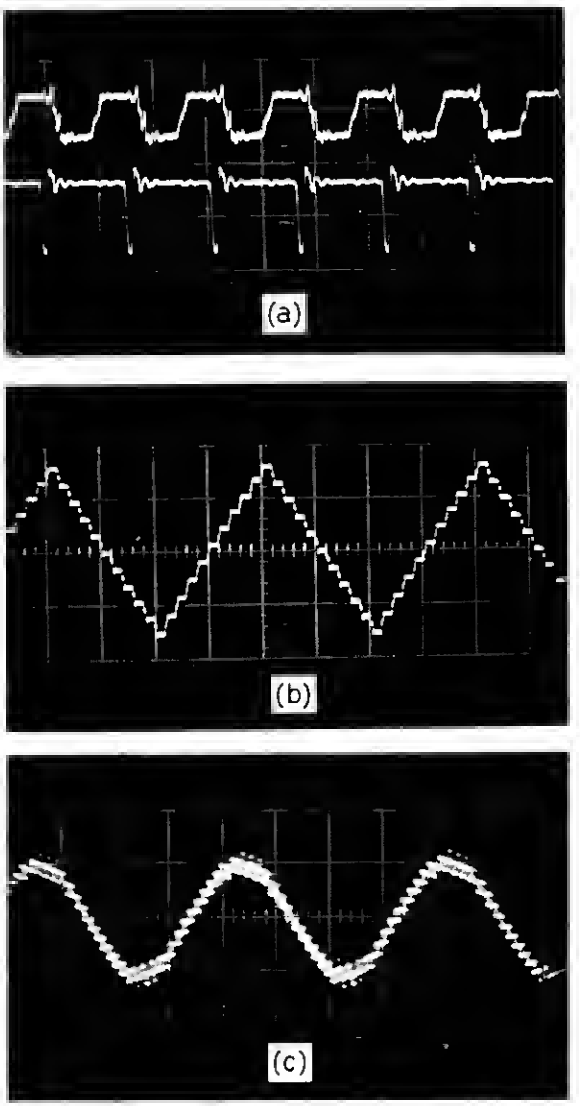

Fig. 9 — (a) Analog output $y(t)$ and digital output with no input (100 ns/cm); (b) $y(t)$ with system in overload (400 ns/cm); (c) $y(t)$ with system not in overload (2 μs/cm).

results because the frequency of the sine wave is not a submultiple of the sampling frequency.

4.2 *Noise Loading Test*

The use of the noise loading test to measure nonlinearities in a transmission system has been mentioned in Section 1.3. In this test, as shown in Fig. 2, a wideband of gaussian noise is applied to a low-pass filter to band limit the input to the delta modulator. With the switch in the upper position, a narrow band of noise can be eliminated from the input signal. Several band elimination filters are available to cover the input spectrum. This signal is fed into the system and only that band from which signal has been eliminated is allowed to pass to the tuned detector. With the switch in the upper position, only noise introduced by nonlinearities in the delta modulator and uncorrelated with the input is passed into the detector. The power spectrum of the uncorrelated noise component $n(t)$ can be measured by changing the center frequency of the band elimination and bandpass filters. With the switch in the lower position, the full signal enters the system and the tuned detector reads signal and noise within the passband.

4.3 *Cancellation Technique*

To measure the total noise output, $e(t)$, and its spectrum, the arrangement shown in Fig. 10 was set up. The signal is fed to the delta modulator and the output of the delta modulator and the attenuated and delayed input are compared, their difference being the noise introduced by the system.

The immediate problem encountered in this technique is the adjustment of the variable attenuator and the delay to cancel the signal

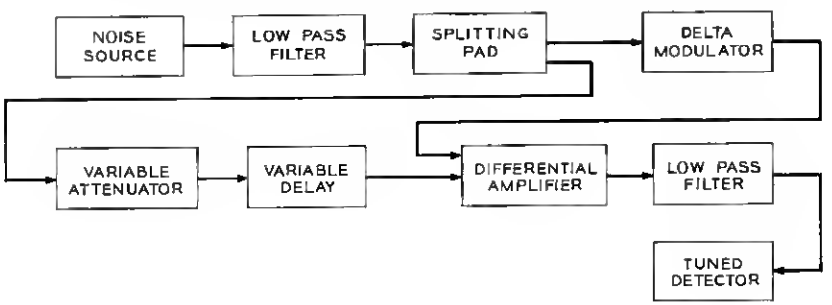

Fig. 10 — Cancellation technique.

component at the output of the delta modulator. The delay is not the same for all frequencies and will have more of an effect at high rather than low frequencies. A sine-wave input whose amplitude was less than that required to overload the system was used to correctly null the system, making the equivalent gain unity. The frequency was chosen as high as conveniently possible (within the signal band) so that the effects of delay could be observed on the nulling procedure. Attenuation and delay were adjusted to produce a null at the input frequency at the tuned detector. Then the noise source was used to replace the sine wave and the output noise measured as a function of frequency by the tuned detector. The gain and delay should be adjusted at each frequency where the noise spectrum is measured. The rather broad null, particularly at the lower frequencies, makes this measurement both tedious and inaccurate. Consequently only the high-frequency approach was used.

The noise-free output signal is measured by removing that input to the difference amplifier that comes from the delta modulator.

4.4 *Accuracy of the Measurements*

The tuned detector used to measure the noise in these experiments was a 37B transmission measuring set. It has a frequency window of about 400 Hz. Therefore, when the noise is measured at a particular frequency, a 400 Hz band is actually measured and the meter reading must be averaged, ignoring peaks. It is estimated that the readings are accurate to about ± 0.5 dB.

Another source of error arises in the determination of the normalized step size kF_s. As mentioned above kF_s can be found from direct measurement on an oscilloscope, or by using a square wave input that overloads the system. A small error in this measurement is equivalent to a displacement in the noise curve (or signal-to-noise ratio) when plotted against kF_s. The noise changes in the overload and granular regions about 1 dB for every dB change in kF_s. Furthermore, the spectrum in overload also changes very rapidly with kF_s.

Therefore, it is fair to conclude that the experimental results in Section V are accurate to about ± 1 dB.

V. RESULTS

5.1 *Noise Loading Results—Uncorrelated Noise Component*

In Fig. 11 we have plotted the spectrum of the signal uncorrelated component of the noise as obtained by the noise loading test for three

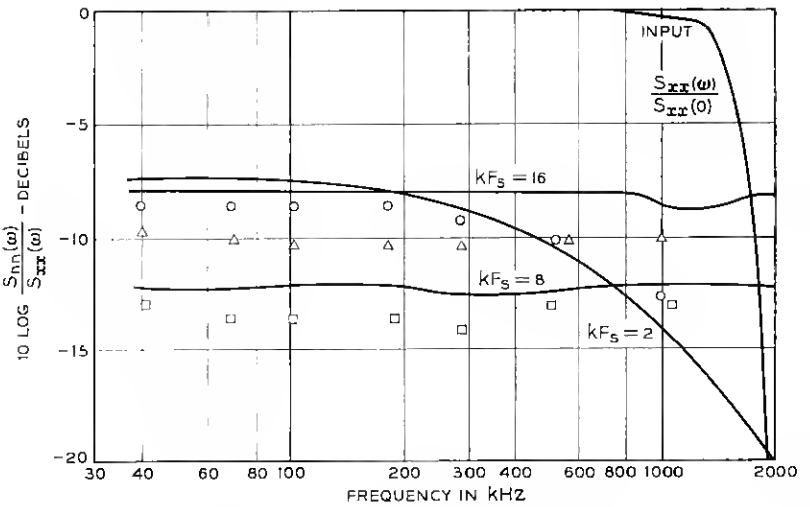

Fig. 11 — Δ-mod uncorrelated noise spectrum, $F_s = 8$.
○ $kF_s = 2$
□ $kF_s = 8$
◇ $kF_s = 16$
— computer results.

values of kF_s. For $kF_s = 8$ and 16 notice that the noise spectrum is flat, as expected, since granular noise is predominant. When $kF_s = 2$, overload noise is controlling, and the noise spectrum is largest at low frequencies. Agreement between the computer generated spectrum and the measured spectrum is good except where the granular noise is small. In this region, it is believed that round-off errors in the computer simulation account for the discrepancy. Integration of the noise spectrum yields the signal to noise curve of Fig. 12 plotted as a function of kF_s.

5.2 *Cancellation Technique—Total Noise*

Noise spectrum measurements obtained by the cancellation technique are compared with computer results in Fig. 13. As before, for $kF_s = 8$ and 16 the spectrum is flat and nearly identical in level with the noise loading results. When well into overload ($kF_s = 2$), the total noise spectrum peaks at the high frequency end. This behavior is readily explained in terms of our equivalent linear system. Consider the difference $e(t)$ between the input signal and the output of the

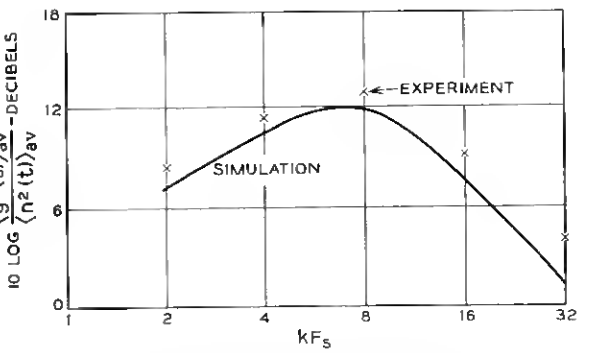

Fig. 12 — Δ-mod signal to uncorrelated noise ratio, $F_s = 8$.

equivalent linear system of Fig. 3

$$e(t) = x(t) - y(t) = x(t) - n(t) - \int_{-\infty}^{\infty} g(t - \tau)x(\tau)\, d\tau \tag{15}$$

or

$$e(t) = \int_{-\infty}^{\infty} [\delta(t - \tau) - g(t - \tau)]x(\tau)\, d\tau - n(t). \tag{16}$$

Since $n(t)$ and $x(t)$ are uncorrelated by definition, it is an easy matter to show that the error spectrum of the total noise is

$$S_{ee}(\omega) = S_{nn}(\omega) + |\, 1 - G(j\omega)\,|^2 S_{xx}(\omega). \tag{17}$$

Substituting $H(j\omega)$, obtained by statistical linearization and given in equation (10) for the equivalent linear system function $G(j\omega)$ in equation (17), we get

$$S_{ee}(\omega) = S_{nn}(\omega) + \frac{\dfrac{\omega^2}{\omega_c^2}}{1 + \dfrac{\omega^2}{\omega_c^2}} S_{xx}(\omega). \tag{18}$$

From either equation (17) or (18) we can see that when $G(j\omega)$ is essentially unity (in the granular region) that the total noise is given by $S_{nn}(\omega)$. On the other hand, when well into overload, the low frequency portion of the total noise is determined by $S_{nn}(\omega)$ and the noise at high frequencies increases due to the second term in equation (18), the term linearly dependent on the input. Indeed, we can use the measured noise spectrum in Fig. 13 for $kF_s = 2$ along with equa-

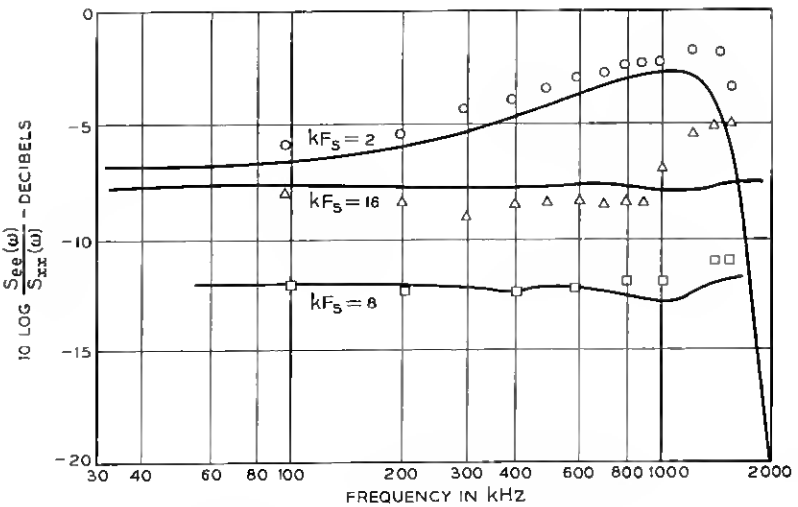

Fig. 13 — Δ-mod error spectrum, cancellation technique, $F_s = 8$.
○ kF$_s$ = 2
□ kF$_s$ = 8
◇ kF$_s$ = 16
— computer results.

tion (18) to determine the corner frequency for the equivalent linear system. The f_o so obtained is about 0.4 f_b in agreement with the analysis.

For completeness, we present in Fig. 14 the signal-to-total-noise ratio obtained by integrating the curves of Fig. 13. In addition, we have noted the corresponding analytical results obtained by using the

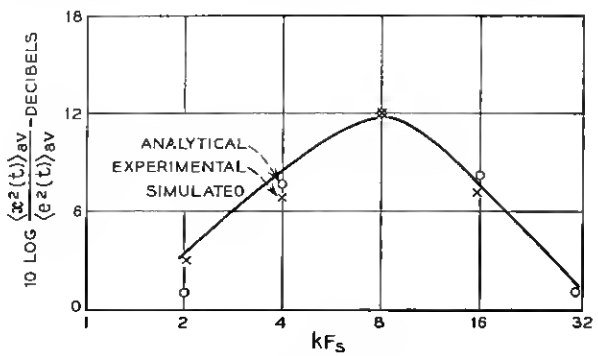

Fig. 14 — Δ-mod signal to error ratio, cancellation technique, $F_s = 8$.

results of Refs. 9 and 10. Agreement is good except when far into the overload region where it is known that the mean square value of the total noise obtained analytically is a coarse upper bound.

VI. ACKNOWLEDGMENT

We are indebted to R. W. Stroh for his initial efforts in the development of the computer program.

APPENDIX A

Statistical Linearization

A.1 *General*

In this appendix we consider the delta modulation system under pure slope overload conditions. Our objective is to replace the hard limiter in the encoder loop with a linear amplifier. We give three methods for the determination of the gain in this linear approximation.

A.2 *Conventional Statistical Linearization—Gaussian Assumption*

First, we use the statistical linearization method attributed to Booton.[18] We isolate the hard-limiter in Fig. 4 with input $e(t)$ and output $z[e(t)]$ in order to replace it with an ideal linear amplifier of gain K_{eq}. This gain factor is chosen such that $K_{eq}e(t)$ differs least in the mean square sense from $z[e(t)]$. It is readily shown the optimum K_{eq} satisfies

$$K_{eq} = \frac{\langle ez \rangle_{av}}{\langle e^2 \rangle_{av}}. \tag{19}$$

For the hard limiter, under the assumption that $e(t)$ is gaussian, we get the well known result[14]

$$K_{eq} = x_0' \left(\frac{2}{\pi \langle e^2 \rangle_{av}} \right)^{\frac{1}{2}} \equiv K_1 . \tag{20}$$

A.3 *Removal of Gaussian Assumption*

In general, $e(t)$ will not be gaussian; though this is commonly assumed in all references to the statistical linearization method. We remove this assumption in this section since we can determine both $\langle ez \rangle_{av}$ and $\langle e^2 \rangle_{av}$ using the approach given in Ref. 9. Since $\langle e^2 \rangle_{av}$ was found in that reference, we need only consider $\langle ez \rangle_{av} = R_{ez}(0)$.

Notice that when

$$\left.\begin{aligned} e(t) > 0, \quad & z(t) = x_o' \\ e(t) < 0, \quad & z(t) = -x_o' \end{aligned}\right\}. \tag{21}$$

and where

Hence

$$\langle ez \rangle_{av} = x_0' \langle | \, e(t) \, | \rangle_{av} = x_0' \text{ ave } [e(t)] \, |_{p.b.} \tag{22}$$

that is, the average of $e(t)$ over the positive bursts (p.b.) only of tbe slope overload noise.

Following the procedure developed in Ref. 9, we obtain

$$x_0' \langle | \, e(t) \, | \rangle_{av} = \frac{1}{\pi} \frac{b_1^{\frac{1}{2}}}{b_2^{\frac{1}{2}}} \left[\frac{3b_1^{\frac{1}{2}}}{x_0'} \right] \exp \left[- \frac{(x_0')^2}{2b_1} \right] \Omega(\chi_1) \tag{23}$$

where

$$\begin{aligned} \chi_1 &= \frac{x_0' \sqrt{2}}{3(b_1)^{\frac{1}{2}}} \\ \Omega(\chi_1) &= 1 - (1 - \chi_1^2) \exp \left(- \frac{\chi_1^2}{2} \right) - \chi_1^3 \Phi(\chi_1) \\ \phi(\chi_1) &= \int_{\chi_1}^{\infty} \exp \left(- \frac{z^2}{2} \right) dz \\ b_n &= \int_{-f_o}^{f_o} \omega^{2n} S_{xx}(\omega) \, df. \end{aligned} \tag{24}$$

In Ref. 9 it was found that

$$\langle e^2(t) \rangle_{av} = \frac{1}{4(2\pi)^{\frac{1}{2}}} \left(\frac{b_1^2}{b_2} \right) \left(\frac{3b_1^{\frac{1}{2}}}{x_0'} \right)^5 \exp \left\{ - \left[\frac{(x_0')^2}{2b_1} \right] \right\} A(\chi) \tag{25}$$

where $A(\chi)$ is given in equation (66) of Ref. 9. Hence

$$K_{eq} = 4 \left(\frac{2}{\pi} \right)^{\frac{1}{2}} \left(\frac{b_2}{b_1} \right)^{\frac{1}{2}} \left(\frac{x_0'}{3b_1} \right)^3 \frac{\Omega(\chi_1)}{A(\chi)} \triangleq K_2 \, . \tag{26}$$

A.4 *Equivalent Gain from Definition of Equivalent Linear System*

Among the many other viewpoints that might be adopted to find K_{eq}, we single out one that makes use of the definition of the equivalent linear system given in the text. Recall that

$$G(j\omega) \equiv \frac{S_{yx}(\omega)}{S_{xx}(\omega)} = 1 - \frac{S_{ex}(\omega)}{S_{xx}(\omega)} \tag{27}$$

or

$$S_{ex}(\omega) = S_{xx}(\omega) - G(j\omega)S_{xx}(\omega). \tag{28}$$

If we integrate equation (27) over $(-2\pi f_o$ to $+2\pi f_o)$ and choose $G(j\omega) = K_3/K_3 + j\omega$, we obtain the following equation defining K_3.

$$\langle x(t)e(t)\rangle_{av} = R_{ex}(0) = \langle x^2(t)\rangle_{av} - \frac{1}{2\pi}\int_{-2\pi f_o}^{2\pi f_o} \frac{S_{xx}(\omega)}{1 + j\dfrac{\omega}{K_3}}\, d\omega. \tag{29}$$

Noticing that $S_{xx}(\omega)$ is an even function of ω, using

$$F(f) = 2S_{xx}(2\pi f) \quad \text{for} \quad f > 0, \tag{30}$$

and defining $f_c = K_3/2\pi$, we get

$$h(f_c) = \int_0^{f_o} \frac{F(f)\, df}{1 + \left(\dfrac{f}{f_c}\right)^2} = \langle x^2(t)\rangle_{av} - \langle x(t)e(t)\rangle_{av}. \tag{31}$$

The left side of equation (31) is a function of f_c only, and hence of K_3, while the right side of equation (30) is known; a formula for $\langle x(t)e(t)\rangle_{av}$ has been found.[17] Equation (31) can be shown to always have a solution.

A little reflection will convince the reader that equation (31) could have been obtained from scratch by preselecting the form of the equivalent linear system, and requiring that $x(t)$ be uncorrelated with $n(t)$ at $\tau = 0$. The approach we have taken could be generalized to match various spectral moments of the processes under consideration. This would entail multiplying equation (28) by ω^{2n} prior to integration and choosing the number of parameters in $G(j\omega)$ equal to the number of moments matched. In general a set of simultaneous nonlinear equations would have to be solved and quantities such as $\langle d^n x(t)/dt^n e(t)\rangle_{av}$ obtained using the techniques of Ref. 9. Fortunately, no such generalization is required. As we see below and from Table I all of the techniques used in this Appendix give good agreement with computer simulation.

Example: Application of equation (31) to flat band limited signals $\langle x^2\rangle_{av} = 1, f_o = 1$ gives

$$h(f_c) = \int_0^1 \frac{df}{1 + \left(\dfrac{f}{f_c}\right)^2} = f_c \tan^{-1}\left(\frac{1}{f_c}\right) = 1 - \langle xe\rangle_{av}. \tag{32}$$

APPENDIX B

Harmonic Response of a Delta Modulator with a Leaky Integrator Under Pure Slope Overload Conditions

B.1 *Introduction*

Consider the single-integration delta modulator with a leaky integrator under pure slope overload conditions. The problem is to find the steady-state response of this nonlinear system to a sinusoidal input. The analysis is applicable to differential pulse code modulation and delta modulation with a more complicated linear network in the feedback path.

Consider a sinusoidal input signal:

$$x(t) = X_o \cos \omega_o t \tag{33}$$

with

$$\omega_o = 2\pi f_o . \tag{34}$$

In the steady-state the output $y(t)$ will be a periodic function of t with period $1/f_0$. The maximum value of the magnitude of the slope of the input sinusoidal signal is clearly equal to $\omega_o X_o$ so that if

$$\frac{\omega_o X_o}{x_o'} \leqq 1 \tag{35}$$

the output will follow the input and we will have

$$y(t) = x(t) = X_o \cos \omega_o t. \tag{36}$$

Suppose now that $x_o' < \omega_o X_o$. In this case slope overload occurs. Call ϕ the value of $\omega_o t - 2n\pi$ (where n is a positive integer) for which slope overload occurs for the first time after the beginning of the nth period. Assuming that we have reached the steady-state, the value of ϕ will be the same for all periods.

Clearly $0 < \phi < \pi/2$. The slope of the input signal at the transition point A (Fig. 15) will be negative and equal to $-X_o\omega_o \sin \phi$. (The second derivative at A is also negative and equal to $-X_o\omega_o^2 \cos \phi$.)

For slope overload to begin at A we should have;† $-\omega_o X_o \sin \phi = -x_o'$, so that

$$\sin \phi = \frac{x_o'}{\omega_o X_o}. \tag{37}$$

† A similar analysis may be made in the asymmetric case, that is, when the positive overloading slope is not equal to the negative overloading slope.

At this transition point the output signal begins to follow an exponential curve such that

$$y(t) = X_o \cos \phi - x_o' \frac{1 - \exp\left(-a \dfrac{\omega_o t - \phi - n\pi}{\omega_o}\right)}{a} \tag{38}$$

as long as $y(t)$ exceeds $x(t)$. The exponential segment ends when $y(t)$ and $x(t)$ once again become equal as shown in Fig. 15. For small leak, the response in overload is clearly linear in time. As long as $|\theta| < \phi$ we have for all n

$$y(t) = \begin{cases} X_o \cos \omega_o t \quad \text{for} \quad \theta + n\pi \leqq \omega_o t \leqq \phi + n\pi \\ (-1)^n X_o \cos \phi + (-1)^{n+1} x_o' \dfrac{1 - \exp\left(-a \dfrac{\omega_o t - \phi - n\pi}{\omega_o}\right)}{a} \\ \qquad \text{for} \quad \phi + n\pi \leqq \omega_o t \leqq \theta + (n \pm 1)\pi \end{cases}. \tag{39}$$

It it easy to show that the region where equation (39) is true may be translated to the condition

$$1 \leqq \frac{\omega_o X_o}{x_o'} \leqq \left\{1 + \frac{\pi^2}{4}\left[\frac{1 - \exp\left(-\dfrac{a\pi}{\omega_o}\right)}{\dfrac{a\pi}{\omega_o}}\right]^2\right\}^{\frac{1}{2}}. \tag{40}$$

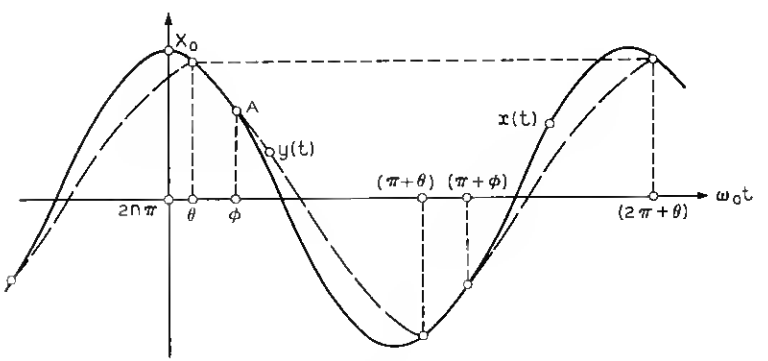

Fig. 15—Slope overload for

$$1 < \frac{\omega_0 x_0}{x_0'} \leqq \left\{1 + \frac{\pi^2}{4}\left[\frac{1 - \exp\ (-a\pi/\omega_0)}{a\pi/\omega_0}\right]^2\right\}^{\frac{1}{2}}$$

(leaky integrator).

In the limit when a goes to zero (no leak) equations (39) and (40) reduce to results obtained previously by Baikovskii.[16] The quantities θ and ϕ coalesce when

$$\frac{\omega_o X_o}{x_o'} \geqq \left\{1 + \frac{\pi^2}{4}\left[\frac{1 - \exp\left(-\frac{a\pi}{\omega_o}\right)}{\frac{a\pi}{\omega_o}}\right]^2\right\}^{\frac{1}{2}} \tag{41}$$

and the output is made up of segments of an exponential curve as shown in Fig. 16. From Fig. 16 we see that

$$\cos \phi_o = x_o' \frac{1 - \exp\left(-\frac{a\pi}{\omega_o}\right)}{2aX_o} \tag{42}$$

and for all n

$$y(t) = (-1)^n x_o' \left\{\frac{1 - \exp\left(-\frac{a\pi}{\omega_o}\right)}{2a} - \frac{1 - \exp\left[-\frac{a}{\omega_o}(\omega_o t - \phi_o - n\pi)\right]}{a}\right\}. \tag{43}$$

Notice that in this case the magnitude of the output depends only on the frequency of the input sinusoidal waveform and not on its

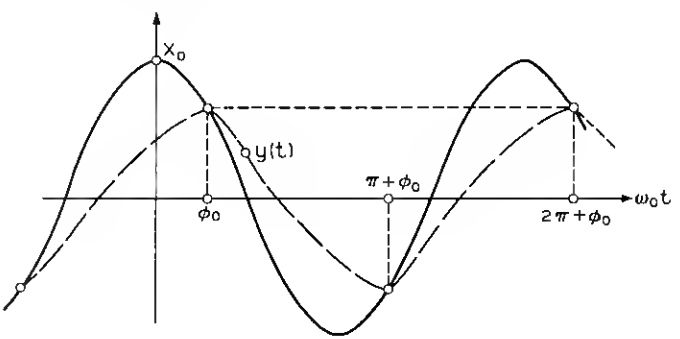

Fig. 16 — Slope overload for

$$\frac{\omega_0 x_0}{x_0'} > \left\{1 + \frac{\pi^2}{4}\left[\frac{1 - \exp\ (-a\pi/\omega_0)}{a\pi/\omega_0}\right]^2\right\}^{\frac{1}{2}}$$

(leaky integrator).

amplitude. Only the phase of $y(t)$ depends on X_o. Clearly when the leak goes to zero ($a = 0$) the response is triangular.

B.2 *Harmonic Analysis of $y(t)$*

In all three regions above the output $y(t)$ is a periodic function of t with period $2\pi/\omega_o$ such that

$$y\left(t + \frac{\pi}{\omega_o}\right) = -y(t). \tag{44}$$

Hence $y(t)$ contains only odd harmonics; it is a straight-forward matter to compute the Fourier coefficients. The complex equivalent gain is given by the ratio of the coefficient of the fundamental in the output to X_o. We leave this manipulation to the interested reader and merely provide a curve of equivalent gain computed for the case of a perfect integrator ($a = 0$), in Fig. 6. Experimental points on the curve are seen to be in close agreement with the analysis.

APPENDIX C

Computational Formulas to Estimate Correlation Function and Spectra

From the sample sequences x_i and e_i for signal and error produced by the simulator, autocorrelation and cross-correlation functions $R_e(j), R_x(j), R_{xe+}(j)$, and $R_{xe-}(j)$ were estimated as the arithmetic means of $e_m e_{m+j}$, $x_m x_{m+j}$, $e_m x_{m+j}$ and $e_m x_{m-j}$, respectively. In the computations, sample sequences of length 10,000 were used. Correlations were computed up to $j = 30$. It is easy to show that spectrum estimates may be obtained by using the correlation estimates as coefficients of a Fourier series. In the case of the cross spectrum, real and imaginary parts must be computed. For clarity, the formulas are listed below. Using the relationship derived in Section 2.1, the uncorrelated noise spectrum may be estimated by:

$$S_n(j) = S_e(j) - \frac{1}{S_x(j)}\left(\{\mathrm{Re}\,[S_{xe}(j)]\}^2 + \{\mathrm{Im}\,[S_{xe}(j)]\}^2\right). \tag{45}$$

To smooth possible ripples in the spectrum estimates due to time truncation of the correlation functions, a hanning window function was used.[19] This smoothing amounts to replacing each spectrum estimate by a linear sum of the estimate and the two adjacent estimates, with weights $\frac{1}{4}$, $\frac{1}{2}$, and $\frac{1}{4}$.

Error spectrum:

$$S_e(j) = R_e(0) + 2 \sum_{l=1}^{N-2} R_e(l) \cos \frac{lj\pi}{N-1} + R_e(N-1) \cos j\pi. \quad (46)$$

Signal spectrum:

$$S_x(j) = R_x(0) + 2 \sum_{l=1}^{N-2} R_x(l) \cos \frac{lj\pi}{N-1} + R_x(N-1) \cos j\pi. \quad (47)$$

Cross spectrum:

$$\text{Re}\,\{S_{xe}(j)\} = R_{xe}(0) + \sum_{l=1}^{N-2} [R_{xe+}(l) + R_{xe-}(l)] \cos \frac{lj\pi}{N-1} + \tfrac{1}{2}[R_{xe+}(N-1) + R_{xe-}(N-1)] \cos j\pi \quad (48)$$

$$\text{Im}\,\{S_{xe}(j)\} = \sum_{l=1}^{N-2} [R_{xe+}(l) - R_{xe-}(l)] \cos \frac{lj\pi}{N-1}. \quad (49)$$

REFERENCES

1. Deloraine, E. M., Van Merlo, S., and Derjavitch, B., "Method and System of Impulse Transmission," French Patent No. 932–140, August 10, 1946, p. 140.
2. de Jager, F., "Delta Modulation, a Method of PCM Transmission Using 1-Unit Code," Philips Res. Rep. 7, 1952, pp. 442–466.
3. Cutler, C. C., "Differential Quantization of Communications Signals," U.S. Patent No. 2,605,361, applied for June 29, 1950, issued July 29, 1952.
4. Graham, R. E., "Predictive Quantization of Television Signals," IRE Wescon Record, Part IV, August 1958, pp. 147–156.
5. *Special Issue on Redundancy Reduction*, C. C. Cutler, ed., Proc. IEEE, *55*, No. 3 (March 1967).
6. O'Neal, J. B., Jr., "Delta Modulation Quantizing Noise Analytical and Computer Simulation Results for Gaussian and Television Input Signals," B.S.T.J., *45*, No. 1 (January 1966), pp. 117–141.
7. Inose, H., Yasuda, Y., Kawai, Y., and Takagi, M., "Subscriber Line Circuits for an Experimental Time Division Multiplex Exchange System Featuring Delta Modulation Techniques," J. Elec. Commun. Engineers of Japan, *44*, (1961), pp. 1322–1328.
8. Zetterberg, L. A., "A Comparison Between Delta and Pulse Code Modulation," Ericsson Technics, *11*, No. 1 (January 1955), pp. 95–154.
9. Protonotarios, E. N., "Slope Overload Noise in Differential Pulse Code Modulation Systems," B.S.T.J., *46*, No. 9 (November 1967), pp. 2119–2162.
10. Van de Weg, H., "Quantizing Noise of a Single Integration Delta Modulation System with an N-Digit Code," Philips Res. Rep. 8, 1953, pp. 367–385.
11. Bennett, W. R., "Spectra of Quantized Signals," B.S.T.J., *27*, No. 3 (July 1948), pp. 446–472.
12. Schwartz, M., Bennett, W. R., and Stein, S., *Communications Systems and Techniques*, New York: McGraw Hill, Inc., 1966, p. 224.
13. Kazkov, I. Y., "Problems of the Theory of Statistical Linearization and its Applications," Proc. First Int. Congress, Int. Federation of Automatic Control, Moscow, 1960, pp. 717–723.
14. Smith, H. W., *Approximate Analysis of Randomly Excited Nonlinear Controls*, Cambridge, Massachusetts: MIT Press, 1966.

15. Karafin, B. J., "A Sampled-Data Simulation Language," Chapter 8 in *System Analysis by Digital Computer*, Kuo, F. F. and Kaiser, F. F., eds., New York: John Wiley and Sons, 1966, pp. 286–312.
16. Baikovskii, V. M., "Application of the Describing Function Method to the Study of Automatic Unitary Code Systems," Automation and Remote Control, *26*, No. 9 (September 1966), pp. 1494–1504.
17. Protonotarios, E. N., unpublished work.
18. Booton, R. C., Jr., "Nonlinear Control Systems with Random Inputs," Trans. of IRE Professional Group on Circuit Theory, *CT-1*, No. 9 (September 1954).
19. Blackman, R. B., and Tukey, J. W., *The Measurement of Power Spectra*, New York: Dover Publications, Inc., 1958.